

First arrival picking using U-net with Lovasz loss and nearest point picking method

Pengyu Yuan, *University of Houston*; Wenyi Hu, *Advanced Geophysical Technology, Inc*; Xuqing Wu, *Jiefu Chen, Hien Van Nguyen, University of Houston*

Summary

We proposed an improved segmentation and picking workflow to solve the first arrival picking problem for seismic signal processing. Unlike traditional classification algorithm, image segmentation method can utilize the location information by outputting a prediction map which has the same size of the input image. A parameter-free nearest point picking algorithm is proposed to further improve the accuracy of the first arrival picking. The algorithm is test on synthetic clean data, synthetic noisy data, synthetic picking-disconnected data and field data. It performs well on all of them and the picking deviation reaches as low as 4.8ms per receiver.

The first arrival picking problem is formulated as the contour detection problem. Similar to Wu et al. (2019), we use U-net to perform the segmentation as it is proven to be state-of-the-art in many image segmentation tasks. Particularly, a Lovasz loss instead of the traditional cross-entropy loss is used to train the network for a better segmentation performance. Lovasz loss is a surrogate loss for Jaccard index or the so-called intersection-over-union (IoU) score, which is often one of the most used metrics for segmentation tasks. In the picking part, we use a novel nearest point picking (NPP) method to take the advantage of the coherence of the first arrival picking among adjacent receivers. Our model is tested and validated on both synthetic and field data with harmonic noises. The main contributions of this paper are as follows:

- Used Lovasz loss to directly optimize the IoU for segmentation task. Improvement over the cross-entropy loss with regard to the segmentation accuracy is verified by the test result.
- Proposed a nearest point picking post processing method to overcome any defects left by the segmentation output.
- Conducted noise analysis and verified the model with both noisy synthetic and field datasets.

Introduction

In the seismic data processing area, first arrival picking is detecting the first arrivals of refracted signals from all signals received by receiver arrays. It is important but challenging because it is strongly affected by the subsurface structure, signal-to-noise ratio, etc. First arrival picking requires extensive manual interventions by domain experts, which is labor-intensive and time consuming.

Manual picking is a straightforward method but it depends on the experience of experts and the estimation criteria is highly subjective. If the data volume is large, picking may consume a lot of time. The semi-automatic picking method is developed

in order to pick the first arrivals faster(Peraldi and Clement (1972)). However, they tend to fail when the pulse shape changes from trace to trace and when bad or dead traces appear. Automatic first arrival picking methods are always preferred and a variety of these kind of techniques are explored over the decades. Energy ratio based methods may perform badly when the data quality is not good enough(Coppens (1985) Chen and Stewart (2005) Wong et al. (2009)). Another branch of first arrival picking method is to use neural networks. McCormack et al. (1993), Maity et al. (2014), and Mousavi et al. (2016) used the shallow neural network and these methods are highly sensitive to hand-designed features such as STA/LTA ratio, the amplitude, and the frequency.

In recent years, deep learning has achieved great success in many fields, especially for computer vision. The seismic data are also images. Hollander et al. (2018), Yuan et al. (2018), and Duan et al. (2018) use deep neural networks as a classifier, to decide whether there is a first arrival signal or it is a poor picking. Both Tsai et al. (2018) and Wu et al. (2019) formulated the first arrival picking problem as the segmentation problem. It takes advantage of the global information of the image by splitting the image into two parts. The first arrival we want is the edge between the signal area and non-signal area. However, segmentation alone cannot guarantee that the picking results meet the minimum accuracy requirement and post-processing is necessary to fix the residual segmentation defects. A nearest point picking post-processing method is proposed in this paper and it significantly improves the overall performance of the workflow.

Problem Description

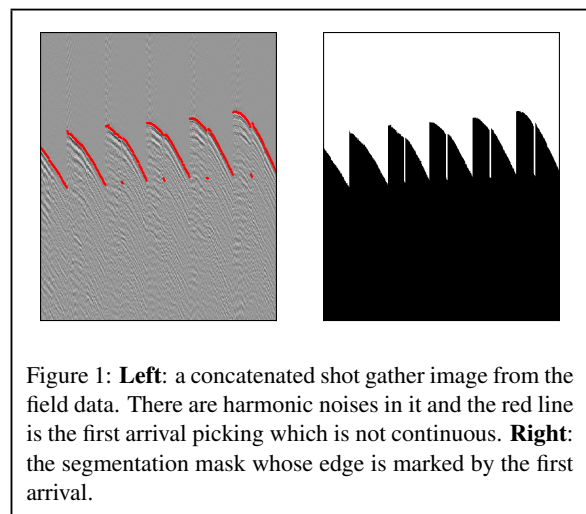


Figure 1: **Left:** a concatenated shot gather image from the field data. There are harmonic noises in it and the red line is the first arrival picking which is not continuous. **Right:** the segmentation mask whose edge is marked by the first arrival.

Figure 1 shows a concatenated shot gather image from the field

SEG abstract example

data and the ground truth segmentation mask. The horizontal axis is different receivers while the vertical axis represents the time. Each column in the image is a trace, representing the response of the seismic signal from a source to a receiver throughout the time steps. The task is to segment the seismic image into two parts and then pick the boundary automatically.

In the ideal case, before the first arrival signal, the receiver should receive no signals. However this is not the case in the field data. The original seismic trace is contaminated by multiple types of noises and they exists in the whole trace. The picking line may also be disconnected because of missing traces or because we want to pick first arrivals for several shots at the same time. The number of receivers is not consistent for each shot gathers. Because harmonic noise radiated from power-line is very typical in seismic data, In this paper, we simulated the harmonic noises and disconnected situations on synthetic data and also tested on the field data to verify the robustness of the proposed model and workflow.

Methodology

U-net

Ronneberger et al. (2015) proposed a convolutional network called U-net with contracting path and expansive path to output segmentation map which has similar dimension with the input image. Both high-level and low-level features are extracted by the downsampling path, the upsampling path, and the skip connections. As shown in Figure 2, the contracting path is composed of 3 blocks. First two blocks are composed of two convolution layers followed by one max pooling layer. The last block only has two convolution layers and it also acts as a bridge to the decoder part. Each convolution layer uses 3×3 kernels. Batch normalization and Relu activation function are used after the convolution layer. The decoder is symmetric to the encoder and it has 2 blocks. Each block is constructed by two convolution layers and one unpooling layer. At the end of the decoder, a 1×1 convolution layer is added to project the 32 feature maps to only 2 classes. And a softmax function is used to map the unnormalized logits to the probabilities. The output segmentation map assigns each single pixel to an area which has or does not have seismic signals.

Loss function

Cross-entropy

One of the most widely used functions in the pixel-wise classification problems is the cross-entropy loss:

$$\text{loss}(\mathbf{f}) = -\frac{1}{N} \sum_{i=1}^N \log f_i(y_i^*) \quad (1)$$

where N is the number of pixels in a batch, $y_i^* \in \{0, 1\}$ is the ground truth class of a pixel i . $y_i^* = 1$ means pixel i is in the signal area. $f_i(y_i^*)$ is the predicted probability of pixel i belongs to class y_i^* . The predicted class for a given pixel i is $\hat{y}_i = \arg \max_{y \in \{0, 1\}} f_i(y)$.

Lovasz hinge loss

Proposed by Berman et al. (2018), the Jaccard index, also

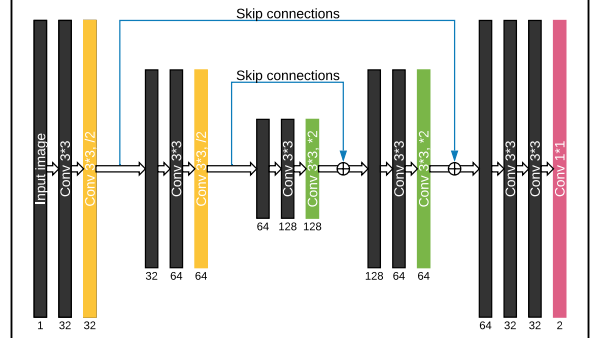


Figure 2: 5-blocks U-net structure. The contracting path has 3 blocks to extract the features, the expansive path has 2 blocks to restore the image size. The number of feature maps are denoted under each layer.

referred to as the intersection-over-union score, is commonly used in the evaluation of semantic segmentation:

$$J_c(\hat{y}, y^*) = \frac{|\{\hat{y} = c\} \cap \{y^* = c\}|}{|\{\hat{y} = c\} \cup \{y^* = c\}|} \quad (2)$$

Then the miss detection is defined as:

$$\Delta_{J_c}(\hat{y}, y^*) = 1 - J_c(\hat{y}, y^*) \quad (3)$$

The ground truth y^* is fixed. If we take the derivative of Δ_{J_c} with regard to the network output $F_i(c)$, the result is either 0 or inf, which makes it impossible to optimize. The Δ_{J_c} can be rewritten as a function of a set of mispredictions m , where the mispredictions is defined as:

$$m_i = \begin{cases} 0, & \text{if } y_i^* = \hat{y}_i \\ 1, & \text{if } y_i^* \neq \hat{y}_i \end{cases} \quad (4)$$

Lovasz hinge loss is an interpolation version of Δ_{J_c} by:

$$\bar{\Delta}_{J_c}(m_{\pi_i}) = \sum_{i=1}^p m_{\pi_i} g_{\pi_i}(\mathbf{m}) \quad (5)$$

where p is the number of samples, π is a permutation ordering of components of \mathbf{m} in decreasing order, i.e. $m_{\pi_1} \geq m_{\pi_2} \dots \geq m_{\pi_p}$. The ground truth label is mapped to $y^* \in \{-1, 1\}$ and misprediction is replaced with the hinge loss for an input image \mathbf{x} :

$$m_{\pi_i} = \max(1 - F_{\pi_i}(\mathbf{x})y_{\pi_i}^*, 0) \in \mathbb{R}^p \quad (6)$$

and the contribution of sample π_i to Δ_{J_c} is given by

$$g_{\pi_i}(\mathbf{m}) = \Delta_{J_c}(\{\pi_1, \dots, \pi_i\}) - \Delta_{J_c}(\{\pi_1, \dots, \pi_{i-1}\}). \quad (7)$$

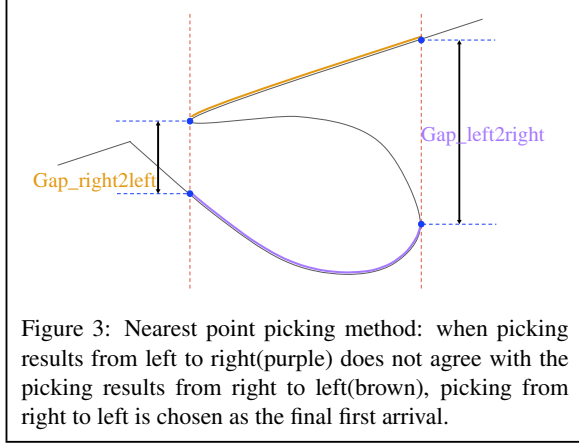
where $\{\pi_1, \dots, \pi_i\}$ means only the first π_i points with highest loss of \hat{y} are used and $\hat{y}_j = y_j^*$ for $j > \pi_i$. Lovasz loss is differentiable with regard to the network output $F(\mathbf{x})$ and it is easy to be plugged into the segmentation model.

Training

We initialize the weights and bias in our networks randomly and use Adam optimizer. The learning rate is 10^{-3} and the training epochs number is 50 with a batch size of 4. The images are normalized before sent to the network. The networks

SEG abstract example

is determined by the kernels in each layer and is independent to the image size, which gives us the flexibility that we do not need to scale or crop the input image again when it comes to the testing time.



Post-processing Picking

first point picking (FPP)

Suppose we have R receivers in one shot gather images. The simplest picking method is for each receiver r , pick the first pixel which is predicted to be a true signal.

$$\hat{t}_r = \arg \min_t \{t | \hat{y}_{(r,t)} = 1\}, \quad r \in [0, R] \quad (8)$$

where (r, t_r) are the coordinates of the selected pixel for receiver r .

nearest point picking (NPP)

For each receiver r , after we get the prediction map from the neural networks, we would get a prediction trace for this particular receiver. Since we know that the first arrival must on the edge, we can find all possible candidates by tracking the edge as follows:

$$t_r \in \{Candidates\}, \quad \text{if } \hat{y}_{(r,t)} - \hat{y}_{(r,t-1)} = 1 \quad (9)$$

After that, we use the correlation of the first arrivals across the traces to select the most reasonable candidate. Given the picking point from the adjacent trace t_{r-1} , the picking point in current trace is selected by

$$\hat{t}_r = \arg \min_{t_r} |t_r - t_{r-1}| \quad \text{for } t_r \in \{Candidates\} \quad (10)$$

One-direction NPP could leads to a biased picking and deviate from the true path due to an imperfect segmentation. To solve the problem, we consider applying NPP from left to right and then from right to left. After getting two picking lines, we compare the difference. If they agree with each other, then the common first arrival is picked. When they disagree, we calculate the gap at the edge of common picking point. As showed in Figure 3 The picking direction with a lower gap wins the competition as the error is likely to be accumulated during the nearest point picking. In other words, we conduct a greedy search on both directions and locate the local minimal based on the segmentation mask.

Datasets	synthetic data	synthetic Disc. data	synthetic noisy data	field data
Model trained on	synthetic data	synthetic data	synthetic data	field data
Acc with CE loss	99.13%	99.09%	98.79%	97.83%
MAE with FPP (ts)	22.56	23.50	26.84	27.54
MAE with NPP (ts)	0.85	4.27	11.66	11.52
Acc with Lovasz loss	99.92%	99.91%	99.18%	98.97%
MAE with FPP (ts)	0.68	0.79	1.65	5.55
MAE with NPP (ts)	0.60	0.79	2.33	4.89
Image size	1250 * 2000	1250 * (1400~2000)	1250 * 2000	750 * (600~700)

Table 1: Seismic image segmentation and picking results on the testing set. Rows 2-4 use cross-entropy loss while rows 5-7 use Lovasz loss (ts is time step)

Experiments

In this section, we evaluate our method on three datasets: synthetic data, noisy and disconnected synthetic data, and field data. Our first arrival picking algorithm performs well on all of them. The results are summarized in Table 1. All of the models have the same structure. We can find that the best model is Unet with Lovasz loss and NPP method.

Metrics

Semantic segmentation can also be considered as a pixel-wise classification task. Thus we can use classification accuracy to measure the performance of our convolutional network. The segmentation accuracy is

$$accuracy(\mathbf{f}) = \frac{1}{mn} \sum_{j=1}^m \sum_{i=1}^n I(\hat{y}_{ij} = y_{ij}^* | f_{ij}) \quad (11)$$

where m is the number of images in a validation set or test set, n is the number of pixels in one image, $I(X)$ is the indicator function, which means it equals 1 if X is true, otherwise 0. f_{ij} is the network prediction for image j at pixel i .

The aforementioned metric alone is not enough since the main focus is the boundary and the classification results of the other pixels are not that important. To measure the boundary directly, we use mean absolute error(MAE)

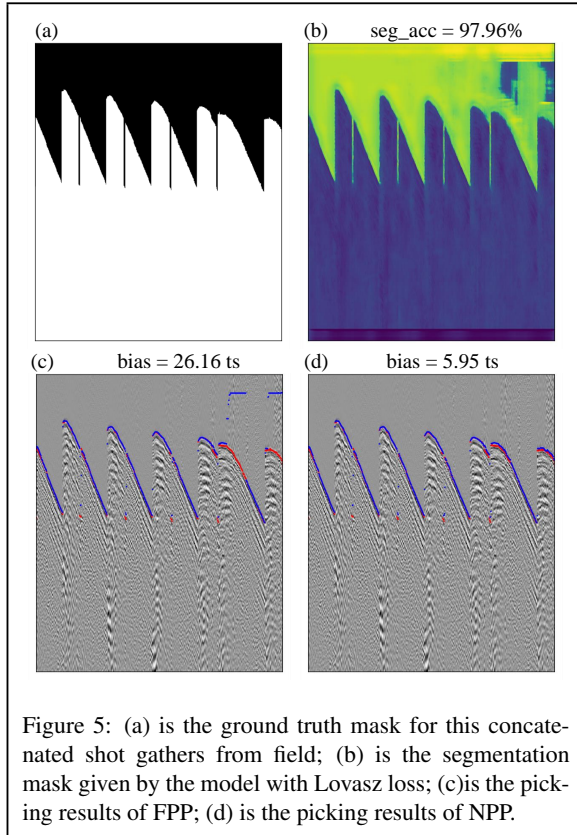
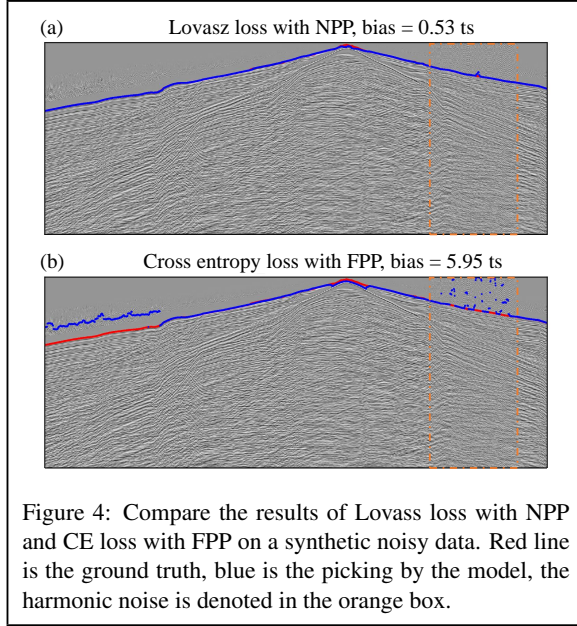
$$MAE(\hat{\mathbf{t}}) = \frac{1}{mR} \sum_{j=1}^m \sum_{r=1}^R |\hat{t}_{jr} - t_{jr}^*| \quad (12)$$

where R is the number of columns in one image, \hat{t}_{jr} is the predicted arrival time of the first signal received by receiver r at shot gather j , t_{jr}^* is the ground truth for that signal. MAE is the core metric we use to measure the performance of our first arrival picking algorithm, the lower the better.

Synthetic seismic data

The first experiment is tested on the synthetic seismic data.

SEG abstract example



The image size is 1250*2000. The sample rate is 8ms. We use cropped images with the width of 600 to train the model. We use 1000 samples for training and 200 samples for validation. The lowest MAE is 0.6, and the average timestamp error is only 4.8ms.

Noisy and disconnected synthetic data

Instead of adding simple incoherent noises such as Gaussian white noise or salt and pepper noise, we performed the spectrum analysis and designed a noise generator to synthesize the multi-harmonic noises that are very typical observed in many field seismic datasets. The amplitude of the noise is modeled by Gaussian random process to simulate the continuity across the traces. The maximal amplitude of noise is set to be half of the maximum signal amplitude. This noise generator was designed based on our observation and analyses of large volume of the field datasets; hence we believe it produces very realistic multi-harmonic noises. In addition, we may also have some images with disconnected first arrival signals due to the missing receivers or spliced shot gathers. Figure 4 proves our model performs well with noisy data or traces with gaps.

Field seismic data

Field data is more complicated compared to synthetic data. The raw data has different size and each image contains several shot gathers. Almost every shot gather is contaminated by the noises. Each field image has a size around 750 * 650. Figure 5 shows that when the segmentation results has mispredictions in the upper area, some noises will be picked as the first arrival if we use FPP method. In contrast, if we use NPP method, the mispredicted picking points will be "pulled down" and the picking results are much close to the groundtruth despite segmentation errors. The algorithm also has the ability to pick small shot gather with width less than 5. The model can be further improved with more training data.

Conclusion

In this paper, we proposed an improved deep learning segmentation method plus a parameter-free post-processing picking method to automatically pick the first arrival signals for the seismic data. We use the latest surrogate IoU loss, Lovasz loss, to train our model. Compared to the cross entropy loss, we proved that Lovasz loss can improve the overall performance. We also test our method with noisy data. Finally, the reliability of the model is validated on field data with high accuracy compared to hand-picking results.

Acknowledgments

This material is based upon work supported by National Science Foundation under Grant No. 1746824

SEG abstract example

Appendix A

The source of the bibliography

```
@article{wu2019semi,
  title={Semi-automatic first arrival picking of micro-seismic events by using pixel-wise convolutional image segmentation method},
  author={Wu, Hao and Zhang, Bo and Li, Fangyu and Liu, Naihao},
  journal={Geophysics},
  volume={84},
  number={3},
  pages={1--70},
  year={2019},
  publisher={Society of Exploration Geophysicists}
}

@article{peraldi1972digital,
  title={Digital processing of refraction data study of first arrivals},
  author={Peraldi, R and Clement, A},
  journal={Geophysical Prospecting},
  volume={20},
  number={3},
  pages={529--548},
  year={1972}
}

@article{coppens1985first,
  title={First arrival picking on common-offset trace collections for automatic estimation of static corrections},
  author={Coppens, F},
  journal={Geophysical Prospecting},
  volume={33},
  number={8},
  pages={1212--1231},
  year={1985},
  publisher={Wiley Online Library}
}

@inproceedings{chen2005multi,
  title={Multi-window algorithm for detecting seismic first arrivals},
  author={Chen, Zuolin and Stewart, R},
  booktitle={Abstracts, CSEG National Convention},
  pages={355--358},
  year={2005}
}

@article{wong2009automatic,
  title={Automatic time-picking of first arrivals on noisy microseismic data},
  author={Wong, Joe and Han, Lejia and Bancroft, J and Stewart, R},
  journal={CSEG. 0 0.2 0.4 0.6 0.8},
  volume={1},
  number={1.2},
  pages={1--4},
  year={2009}
}

@article{mccormack1993first,
  title={First-break refraction event picking and seismic data trace editing using neural networks},
  author={McCormack, Michael D and Zaucha, David E and Dushek, Dennis W},
```

SEG abstract example

```
journal={Geophysics},
volume={58},
number={1},
pages={67--78},
year={1993},
publisher={Society of Exploration Geophysicists}
}

@article{maity2014novel,
  title={Novel hybrid artificial neural network based autopicking workflow for passive seismic data},
  author={Maity, Debotyam and Aminzadeh, Fred and Karrenbach, Martin},
  journal={Geophysical Prospecting},
  volume={62},
  number={4},
  pages={834--847},
  year={2014}
}

@article{mousavi2016seismic,
  title={Seismic features and automatic discrimination of deep and shallow induced-microearthquakes using neural network and logistic regression},
  author={Mousavi, S Mostafa and Horton, Stephen P and Langston, Charles A and Samei, Borhan},
  journal={Geophysical Journal International},
  volume={207},
  number={1},
  pages={29--46},
  year={2016},
  publisher={Oxford University Press}
}

@article{yuan2018seismic,
  title={Seismic waveform classification and first-break picking using convolution neural networks},
  author={Yuan, Sanyi and Liu, Jiwei and Wang, Shangxu and Wang, Tieyi and Shi, Peidong},
  journal={IEEE Geoscience and Remote Sensing Letters},
  volume={15},
  number={2},
  pages={272--276},
  year={2018},
  publisher={IEEE}
}

@incollection{tsai2018first,
  title={First-break automatic picking with deep semisupervised learning neural network},
  author={Tsai, Kuo Chun and Hu, Wenyi and Wu, Xuqing and Chen, Jiefu and Han, Zhu},
  booktitle={SEG Technical Program Expanded Abstracts 2018},
  pages={2181--2185},
  year={2018},
  publisher={Society of Exploration Geophysicists}
}

@incollection{hollander2018using,
  title={Using a deep convolutional neural network to enhance the accuracy of first-break picking},
  author={Hollander, Yaniv and Merouane, Amin and Yilmaz, Orhan},
  booktitle={SEG Technical Program Expanded Abstracts 2018},
  pages={4628--4632},
  year={2018},
  publisher={Society of Exploration Geophysicists}
}
```

SEG abstract example

```
@incollection{duan2018integrating,
  title={Integrating seismic first-break picking methods with a machine learning approach},
  author={Duan, Xudong and Zhang, Jie and Liu, Zhiyang and Liu, Sen and Chen, Zhibo and Li, Weiping},
  booktitle={SEG Technical Program Expanded Abstracts 2018},
  pages={2186--2190},
  year={2018},
  publisher={Society of Exploration Geophysicists}
}

@inproceedings{ronneberger2015u,
  title={U-net: Convolutional networks for biomedical image segmentation},
  author={Ronneberger, Olaf and Fischer, Philipp and Brox, Thomas},
  booktitle={International Conference on Medical image computing and computer-assisted intervention},
  pages={234--241},
  year={2015},
  organization={Springer}
}

@inproceedings{berman2018lovasz,
  title={The Lovász-softmax loss: a tractable surrogate for the optimization of the intersection-over-union measure in neural networks},
  author={Berman, Maxim and Rannen Triki, Amal and Blaschko, Matthew B},
  booktitle={Proceedings of the IEEE Conference on Computer Vision and Pattern Recognition},
  pages={4413--4421},
  year={2018}
}
```

REFERENCES

- Berman, M., A. Rannen Triki, and M. B. Blaschko, 2018, The Lovász-softmax loss: a tractable surrogate for the optimization of the intersection-over-union measure in neural networks: *Proceedings of the IEEE Conference on Computer Vision and Pattern Recognition*, 4413–4421.
- Chen, Z., and R. Stewart, 2005, Multi-window algorithm for detecting seismic first arrivals: Abstracts, CSEG National Convention, 355–358.
- Coppens, F., 1985, First arrival picking on common-offset trace collections for automatic estimation of static corrections: *Geophysical Prospecting*, **33**, 1212–1231.
- Duan, X., J. Zhang, Z. Liu, S. Liu, Z. Chen, and W. Li, 2018, Integrating seismic first-break picking methods with a machine learning approach, *in* SEG Technical Program Expanded Abstracts 2018: Society of Exploration Geophysicists, 2186–2190.
- Hollander, Y., A. Merouane, and O. Yilmaz, 2018, Using a deep convolutional neural network to enhance the accuracy of first-break picking, *in* SEG Technical Program Expanded Abstracts 2018: Society of Exploration Geophysicists, 4628–4632.
- Maity, D., F. Aminzadeh, and M. Karrenbach, 2014, Novel hybrid artificial neural network based autopicking workflow for passive seismic data: *Geophysical Prospecting*, **62**, 834–847.
- McCormack, M. D., D. E. Zaucha, and D. W. Dushek, 1993, First-break refraction event picking and seismic data trace editing using neural networks: *Geophysics*, **58**, 67–78.
- Mousavi, S. M., S. P. Horton, C. A. Langston, and B. Samei, 2016, Seismic features and automatic discrimination of deep and shallow induced-microearthquakes using neural network and logistic regression: *Geophysical Journal International*, **207**, 29–46.
- Peraldi, R., and A. Clement, 1972, Digital processing of refraction data study of first arrivals: *Geophysical Prospecting*, **20**, 529–548.
- Ronneberger, O., P. Fischer, and T. Brox, 2015, U-net: Convolutional networks for biomedical image segmentation: *International Conference on Medical image computing and computer-assisted intervention*, Springer, 234–241.
- Tsai, K. C., W. Hu, X. Wu, J. Chen, and Z. Han, 2018, First-break automatic picking with deep semisupervised learning neural network, *in* SEG Technical Program Expanded Abstracts 2018: Society of Exploration Geophysicists, 2181–2185.
- Wong, J., L. Han, J. Bancroft, and R. Stewart, 2009, Automatic time-picking of first arrivals on noisy microseismic data: CSEG. 0 0.2 0.4 0.6 0.8, **1**, 1–4.
- Wu, H., B. Zhang, F. Li, and N. Liu, 2019, Semi-automatic first arrival picking of micro-seismic events by using pixel-wise convolutional image segmentation method: *Geophysics*, **84**, 1–70.
- Yuan, S., J. Liu, S. Wang, T. Wang, and P. Shi, 2018, Seismic waveform classification and first-break picking using convolution neural networks: *IEEE Geoscience and Remote Sensing Letters*, **15**, 272–276.